Chemical and Process Engineering: New Frontiers, 2026, 47(1), e120
DOI: 10.24425/cpe.2026.155558

Catalytic oxidation of lean hexane-air and isopropanol-air mixtures using the Ag/Fe_2O_3/cenosphere catalyst in the fluidized bed reactor

Przemysław Migas[1]*, Dariusz Bradło[1], Krystian Leski[1], Jan Wrona[2]

[1] Cracow University of Technology, Faculty of Chemical Engineering and Technology, Warszawska 24, 31-155 Cracow, Poland
[2] Cracow University of Technology, Faculty of Environmental Engineering and Energy, Warszawska 24, 31-155 Cracow, Poland

Abstract
The results of the catalytic oxidation of isopropanol and hexane on Fe_2O_3/cenosphere (Fe_2O_3/C) and Ag/Fe_2O_3/cenosphere ($Ag/Fe_2O_3/C$) catalysts in a fluidized bed reactor are presented. The Fe_2O_3/C catalyst was developed by depositing an Fe_2O_3 layer on cenospheres by chemical vapor deposition of Fe, followed by oxidation of the Fe layer. The $Ag/Fe_2O_3/C$ catalyst was obtained by Ag/Fe ion exchange. The catalysts were analyzed by AAS, XRD, and SEM-EDS methods, and the composition of the gaseous products formed during the process was determined using an FTIR analyzer. Catalytic oxidation of isopropanol and hexane was carried out at temperatures ranging from 200 to 450 °C. Enrichment of the cenosphere coating with Ag significantly improves the catalytic decomposition of isopropanol. The temperature of allmost full conversion of this pollutant to CO_2 in the $Ag/Fe_2O_3/C$ process is approximately 370 °C, while the same decomposition using an Fe_2O_3/C catalyst requires temperatures higher than 450 °C. Analysis of the toxicity of exhaust gases generated during the catalytic conversion of hexane showed that up to 450 °C, the gaseous products produced are more toxic than hexane. However, a decrease in the toxicity of the gaseous products during isopropanol conversion was achieved, both for the Fe_2O_3/C and $Ag/Fe_2O_3/C$ processes.

Keywords
VOC removal, toxicity of oxidation products, fluidization; cenospheres, Ag/Fe_2O_3 catalyst

* **Corresponding author, e-mail:**
przemyslaw.migas@pk.edu.pl

Article info:
Received: 25 August 2025
Revised: 10 November 2025
Accepted: 16 January 2026

1. INTRODUCTION

Volatile organic compounds (VOCs) are pollutants originating from, among others, industrial production, agricultural production, and transport, and refer to compounds that at atmospheric pressure have a boiling point below 250 °C. These compounds have a toxic effect, which poses threats to the environment and health. In addition, they have the ability to absorb infrared radiation, which contributes to the greenhouse effect (He et al., 2019). Removing VOCs from the air is particularly problematic when these compounds are present in low concentrations, which prevents their direct combustion or requires the supply of supporting fuel. Among the methods for eliminating VOC contaminants, besides co-combustion with supporting fuel, the following can be mentioned: adsorption Chauveau et.al., 2013; Jurkiewicz et al., 2023), biofiltration Rybarczyk, 2022; Rybarczyk et al., 2023), and catalytic oxidation. In the catalytic oxidation of VOCs, contaminated air is fed into a post-combustion chamber containing a catalytic bed. The catalytic bed' s function is to lower the temperature of full VOC conversion, thereby reducing the energy required to remove these pollutants.

The process catalysts are based on precious metals, mainly palladium and platinum (He et al., 2012; Kim et al., 2022; Tabakova et al., 2025) or oxide materials, which include catalysts based on Mn, Co, Cu, Ce, etc. (Kang et al., 2020; Miao et al., 2019; Todorova et al., 2012; Żukowski et al., 2023). Selected authors also conducted research using silver as a catalytic material in VOC conversion processes (Guo et al., 2019; Zhang et al., 2020), in addition, the effect of silver and gold enrichment of Fe_2O_3 in the removal of pollutants such as methanol, isopropanol, and toluene was investigated (Scirè et al., 2001).

Most studies on the catalytic conversion of VOCs involve stationary bed reactors, and only few authors have conducted their conversion in a fluidized bed reactor. A disadvantage of the stationary bed process is the heterogeneity of the temperature and concentration distribution within the reactor space. This can be avoided in a fluidized bed reactor due to the bed grains circulation.

In the presented work, a fluidized bed with a core-shell catalysts in the form of cenospheres with a nanometric catalytic coatings, Fe_2O_3 and Ag/Fe_2O_3, was used. Cenospheres are aluminosilicate spheres filled with gases, which lead to a relatively low density (Ranjbar and Kuenzel, 2017). Due to their low density, the use of cenospheres in a fluidized bed reactor reduces the gas volumetric flow rate required to achieve minimum fluidization velocity. Cenospheres with a Fe_2O_3 catalytic coating have been used in combustion processes (Żukowski and Berkowicz, 2019a; Żukowski and Berkowicz, 2019b), in hydrogen production from polyoxymethylene (Berkowicz-Płatek et al., 2024), and in the catalytic oxidation of VOC (Migas et al., 2023).

In the presented work, the influence of silver addition to the Fe_2O_3/C catalytic system on the hexane and isopropanol conversion process was investigated and the toxicity of gases generated in the process of utilization of these components was evaluated.

2. MATERIALS AND METHODS

2.1. Preparation of Fe/C and Fe_2O_3/C

The preparation of cenospheres and the process of coating with an iron layer and subsequent oxidation to iron oxide is described in detail by Migas et al. (2023). Briefly, the 160–200 µm particle fraction was isolated from raw cenospheres (Połaniec Power Plant – Poland) and hydrothermally treated for 30 min in distilled water at 80 °C under constant stirring (500 rpm). This process aimed to remove fine fly ash as well as crushed, porous, and damaged particles. Undamaged cenospheres floating on the water surface were collected and then dried for 12 h at 150 °C. The resulting undamaged cenospheres were coated with an Fe layer using the MO–CVD (metal–organic chemical vapor deposition) method, where the iron precursor was iron (0) pentacarbonyl (Sigma Aldrich, Germany, Schnelldorf). This procedure yielded the Fe/C material, which was subsequently used to prepare two catalysts: Fe_2O_3/C (oxidizing Fe/C in air atmosphere in a muffle furnace at 500 °C, 2 h) and Ag/Fe_2O_3/C.

2.2. Preparation of Ag/Fe_2O_3/C

0.03 mol $AgNO_3$ (p.a., Warchem, Poland) was added to 1 dm^3 of demineralized water at 60 °C and stirred for 1 min (500 rpm). Next, 50 g of iron-coated cenospheres (Fe/C) was added and stirred for 30 min. After this time, the phases were separated, the floating material was collected, washed with 100 ml of demineralized water, and dried (3 h, 105 °C). Subsequently, to obtain iron (III) oxide, calcination was carried out at 500 °C for 2 h. After calcination, the material was purified to remove non-adherent silver particles as well as fine and crushed particles. In order to purify the catalyst, the material was added to 250 cm^3 of demineralized water and left for 12 h. After phase separation, the material was dried (3 h, 105 °C) and sieved again to separate fine particles. As a result, 46.1 g of Ag/Fe_2O_3/C cenospheres with intact walls and a size of 160–200 µm was obtained.

2.3. Catalyst characterization

To determine the metal content of the resulting Fe_2O_3/C and Ag/Fe_2O_3/C catalysts, the samples were mineralized. Approximately 1 g of the ground sample was digested with 20 cm^3 of sulfuric acid (1 + 4 v/v). Iron and silver content in the liquid solutions was determined using a Perkin Elmer AAnalyst 300 instrument using flame atomic absorption spectrometry (F-AAS). Microscopy images were taken using a high-resolution Apreo 2 S LoVac scanning electron microscope (SEM) (Thermo Fisher Scientific), equipped with energy-dispersive X-ray spectrometers (EDS detectors) and a backscattered electron (BSE), and secondary electron (SE) detection system. Phase composition was analyzed using a SmartLab SE (Rigaku) powder X-ray diffractometer equipped with a Hypix 400 two-dimensional semiconductor X-ray detector. The diffractometer was operated with the ICDD PDF-4 database. Scanning was performed in the range of 10–80 ° 2θ with a step size of 0.02 ° and a scanning rate of 3.00 °/min.

2.4. Experimental stand and methodology of catalytic tests

The experimental stand of catalytic conversion of VOCs in a fluidized bed reactor has been described in detail in Migas et al. (2023). Briefly 40 g of catalyst (Fe_2O_3/C or Ag/Fe_2O_3/C) with a particle fraction of 160–200 µm was introduced into a glass reactor with an internal diameter of 3.4 cm. The bed was fluidized with air at a volume flow rate of 0.5 dm^3/min contaminated with VOC – hexane at an initial concentration of 2700 ppm or isopropanol at an initial concentration of 3500 ppm. The catalytic conversion process was conducted in the range of 200–450 °C, with a constant temperature increase of 3 °C/min. The composition of the gaseous products generated in the process was monitored using an FTIR analyzer (atmosFIR, Protea, UK, Middlewich). The high resolution of the analyzer ($\sim$ 1 cm^{-1}) allowed for the acquisition of detailed IR spectra of the gas products at 20 s intervals. Based on the FTIR spectra obtained during the process, the concentrations of gaseous components were determined by deconvolution based on reference spectra. The deconvolution process was performed in wavenumber ranges of 850–1350 cm^{-1}, 1900–2300 cm^{-1}, and 2600–3200 cm^{-1}, respectively (Fig. 1). The wavenumber ranges were selected to include the spectra of CO, CO_2, and hydrocarbons, while omitting regions dominated by water vapor. The concentrations of the resulting gaseous products were then converted to mass fractions of carbon derived from a given component.

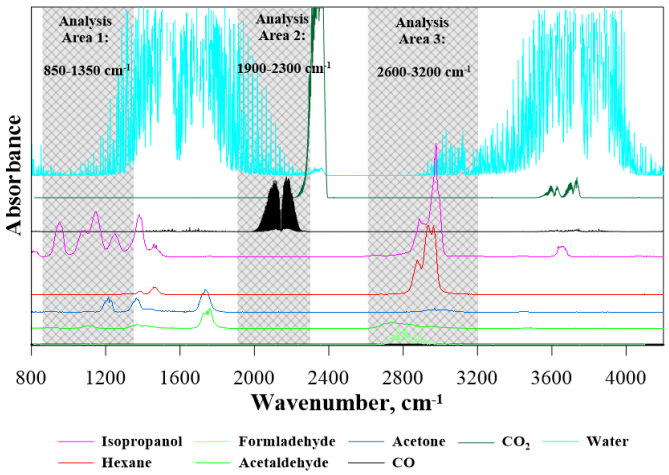

Figure 1. Reference spectra of the analyzed compounds along with the analysis areas.

2.5. Methodology of toxicity tests

In the combustion of organic pollutants, the issue of toxicity is particularly important, as the process should be carried out so that the products formed are less toxic than the original compounds. To determine the toxicity of gases, a methodology described by Rybiński et al. (2021) was adopted. To compare the toxicity of the gases produced, threshold concentration values of gaseous components were applied based on universal values TLV®–TWA (Threshold Limit Values in order of 8-hour time weighted averages, mg/m^3), which specify the maximum permissible concentration that does not cause negative health effects after 8 hours of exposure in the workplace (ACGIH, NIOSH, OSHA).The toxicometric index determined in this way is defined as the standardized volume of toxic gases (in m^3) released from 1 g of the tested sample:

$$W = \frac{E \cdot 1000}{TLV - TWA} \quad (1)$$

where "E" is the specific emission of the component, obtained from the measured data, g/g.

In a continuous gas-phase process, specific emission can be expressed as the ratio of the volume of a given gas component to the total mass of the gases produced. The toxicometric index is then expressed in units of "m^3/g of gas". The sum of the toxicometric indices for all analyzed gas components is calculated and designated as E_T (toxicity – m^3/g of gas). Hence, the higher the value of E_T, the more toxic the exhaust gases released in the process.

2.6. Heat balance calculation

In order to evaluate the energy efficiency of the process depending on the utilized pollutant and catalyst type, appropriate heat balance calculation was carried out. The heat generated during selected compound oxidation $Q_{\text{React.}}(t)$ was calculated according to Eq. (2) as the difference between the products and substrates heat of formation.

$$Q_{\text{React.}}(t) = \left(\sum \Delta_f H^o_{\text{gas}\,i} \cdot \dot{m}_i(t)\right)_{\text{Prod.}} - \left(\sum \Delta_f H^o_{\text{gas}\,i} \cdot \dot{m}_i(t)\right)_{\text{Sub.}} (W) \quad (2)$$

Based on heat generated during reaction and the heat required to preheat introduced air, the γ coefficient was calculated representing the energy demand, according to Eq. (3).

$$\gamma = \frac{Q_{\text{React.}}(t)}{C_{p\,\text{Air}}(T) \cdot \dot{m}_{\text{Air}} \cdot (T(t)_{Bed} - 25°\text{C})} \times 100\% \quad (3)$$

Selected physical and thermodynamic data were obtained from NIST Chemistry WebBook and Engineering ToolBox. During the calculation of γ adiabatic conditions were adopted and the heat capacity of the catalyst was not considered since steady state condition was assumed i.e. catalyst reached intended temperature.

3. RESULTS AND DISCUSSION

3.1. AAS, SEM and EDS analysis of catalysts

F-AAS elemental composition analyses of the samples showed that the Fe_2O_3/C catalyst contained 6.22 wt.% iron. The process of iron-silver ion exchange led to an Ag/Fe_2O_3/C catalyst with 0.33 wt.% Ag and 5.32 wt.% Fe. Fig. 2 shows SEM micrographs of the cenosphere with catalyst layer and the results of EDS elemental composition analysis. Figs. 2A, C, and E show the cenosphere with the Fe_2O_3 catalytic coating, while Figs. 2B, D, and F show the cenosphere with the Ag/Fe_2O_3 catalyst. Both cenosphere particles have a highly porous surface, but their morphology is not related to the presence of catalytic coatings. The resulting iron oxide coating is visible only in EDS analysis (Fig. 2E), which indicates a uniform distribution of fine iron phase grains on the cenosphere surface. Ag particles form larger agglomerates of grains or take the form of sheets with sizes up to several micrometers (Fig. 2F), the distribution of silver is less uniform, but Ag covers almost the entire surface of the cenosphere.

3.2. XRD analysis of Ag/Fe_2O_3/C catalyst

Additional confirmation of the presence of active components Ag and Fe_2O_3 was obtained by XRD analysis (Fig. 3). Characteristic diffraction peaks of Ag were observed at $2\theta = 38.09°$, 44.29°, 64.41°, 77.36° with cubic structure, while Fe_2O_3 occurred in the form of hematite with characteristic reflections at $2\theta = 24.15°$, 33.16°, 35.58°, 40.80°, 49.41°, 53.99°, 62.43°, 63.96° with tetragonal structure. Additionally, the analysis revealed the presence of quartz (SiO_2) and mullite, which are the components of the cenosphere material.

3.3. Results of fluidization test

In order to evaluate the possibility of using the catalyst in the fluidized bed reactor the fluidization tests were conducted. Tests were done at the same reactor where the catalytic oxidation process was performed. In the tests 35 g of catalyst was used, and a pressure sensor (MPXV4006DP) was located beneath the perforated bottom of the reactor. Fig. 4A shows the results of pressure drop as a function of linear velocity of the supplied air for the Fe_2O_3/C and Ag/Fe_2O_3/C materials. The minimum fluidization velocities at room temperature were $\sim$ 1 cm/s for both catalysts. These values are consistent with the results obtained from the Wen-Yu equation (Wen and Yu, 1966), in which the $u_{mf} = 1.02$ cm/s was calculated for inert cenospheres i.e. without catalytic coating (density $d = 788$ kg/m^3, mean particle diameter $d_M = 0.18$ mm, at $T = 25$ °C), so inert cenospheres were used as model material for further calculation. Fig. 4B shows the calculated values of u_{mf} and u/u_{mf} ratio obtained from the Wen Yu equation for inert cenospheres. The minimum fluidization velocity varies in

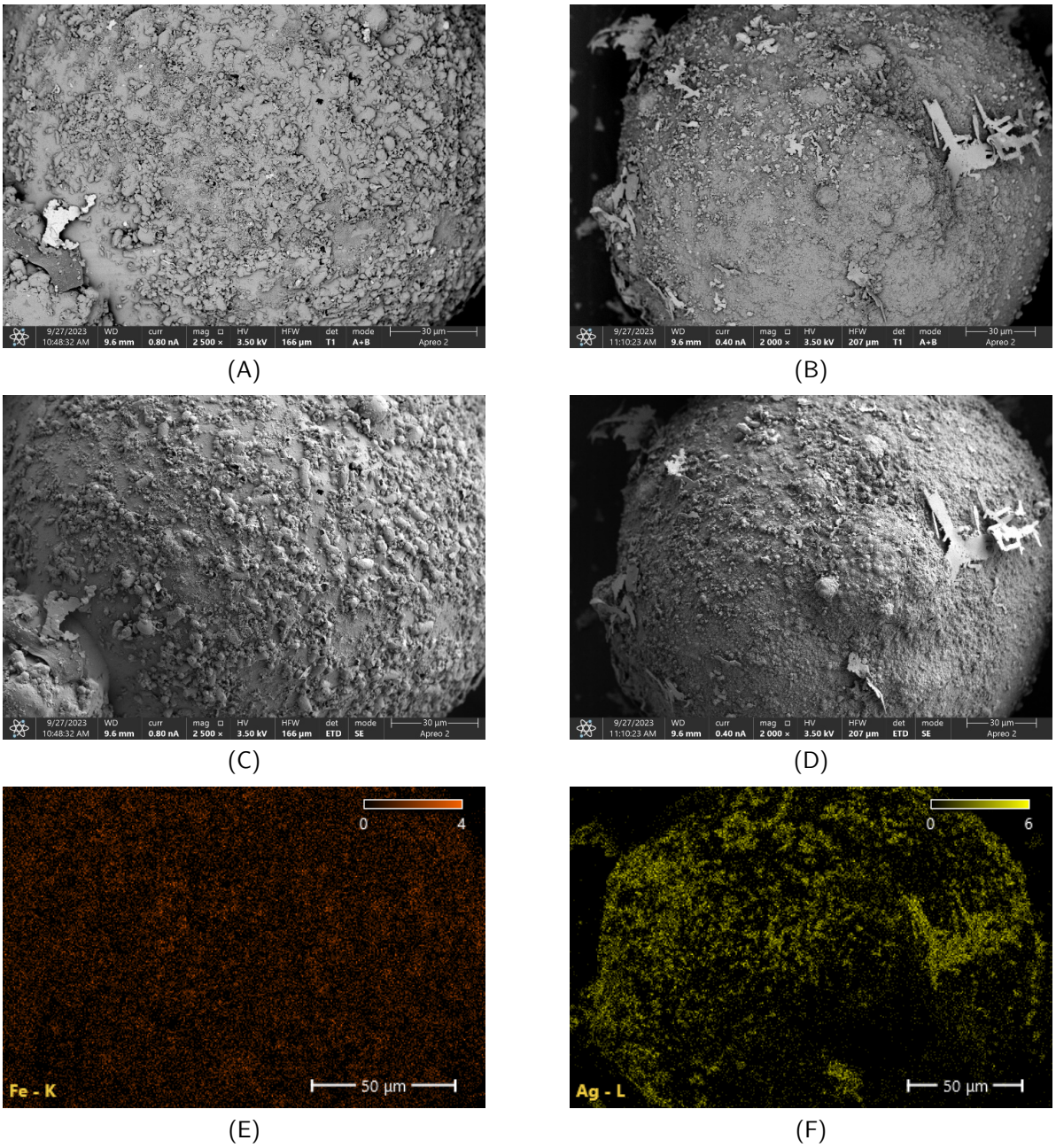

Figure 2. Results of SEM analysis of catalyst layer: A) Fe_2O_3/C – T1 detector; B) Ag/Fe_2O_3/C – T1 detector; C) Fe_2O_3/C – ETD detector; D) Ag/Fe_2O_3/C – ETD detector; E) Fe_2O_3/C – EDS; F) Ag/Fe_2O_3/C – EDS.

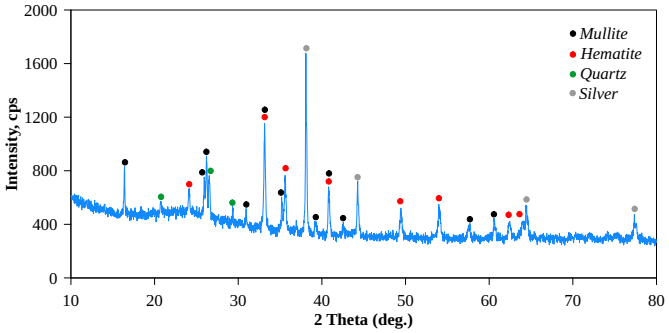

Figure 3. XRD pattern of Ag/Fe_2O_3/C catalyst.

the range of 0.52–1.02 cm/s while the value of u/u_{mf} changes between 0.90–4.33 for $T = 25\,^{\circ}C$ and $450\,^{\circ}C$, respectively. These low u_{mf} and high u/u_{mf} values indicate that the tested catalytic bed is ideally suited for fluidized bed applications. For comparison, the most commonly used material, quartz sand with the density of 2650 kg/m^3 and $d_M = 0.18$ mm has values of $u_{mf} = 3.1$ cm/s and $u/u_{mf} = 0.27$, at $25\,^{\circ}C$, and $u_{mf} = 0.92$ cm/s and $u/u_{mf} = 0.52$ for $450\,^{\circ}C$ (Wenand Yu, 1966). This means that in the case of fluidization of sand, at least twice of the volumetric rate of introduced air is needed.

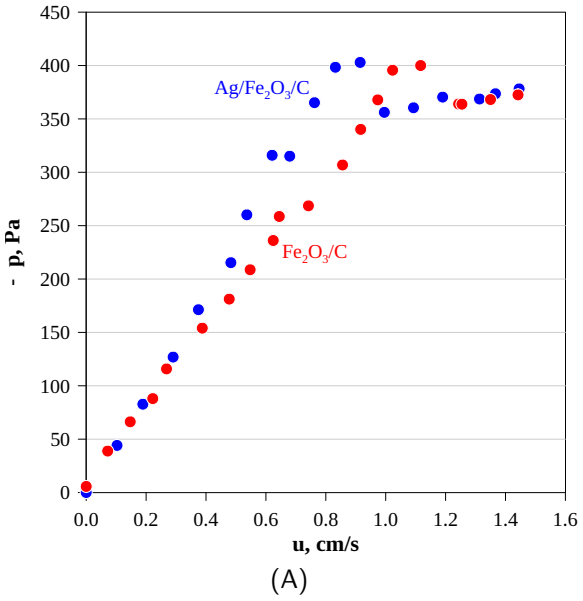

Figure 4. Results of fluidization tests: A) pressure drop for Fe_2O_3/C and Ag/Fe_2O_3/C catalysts; B) minimum fluidization velocity and u/u_{mf} ratio as a function of bed temperature.

3.4. Results of catalytic test

Figures 3 and 6 show selected FTIR spectra of gaseous products obtained during the catalytic conversion of isopropanol and hexane using an Ag/Fe_2O_3/C bed. During the conversion of isopropanol at 250 °C (Fig. 5), the gaseous products include the introduced pollutant with the components of complete decomposition, i.e., carbon dioxide and water, as well as products of incomplete conversion such as acetone and carbon monoxide. The latter exhibit absorbance in the range of 2000–2200 cm^{-1} (CO) and 2800–3150 cm^{-1} (acetone). Although detailed spectral deconvolution also revealed the presence of formaldehyde and acetaldehyde, their concentrations at this temperature were low.

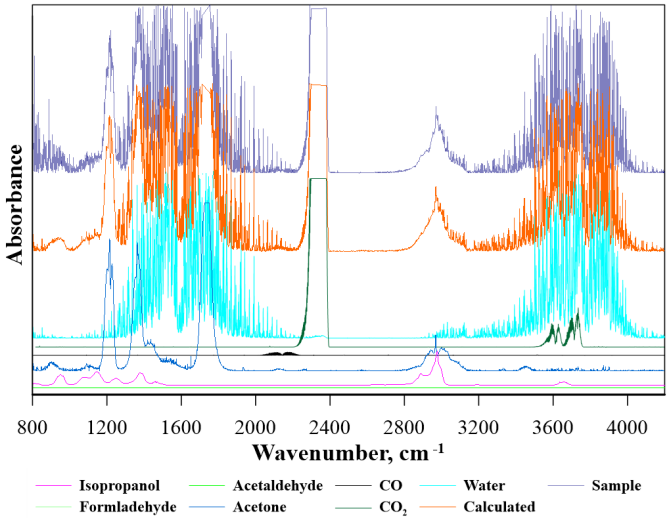

Figure 5. FTIR spectra during catalytic conversion of isopropanol on Ag/Fe_2O_3/C catalyst at 250 °C.

During the conversion of hexane at 350 °C (Fig. 6), the main intermediate decomposition products detected were carbon monoxide and acetaldehyde. Similarly to isopropanol, spectral deconvolution also revealed the presence of formaldehyde. Spectral analysis during tests using an Fe_2O_3/C bed did not reveal other gaseous components, which indicates a similar mechanism of compound decomposition using both types of catalysts. However, the implementation of silver infuenced the concentrations of the gaseous products depending on the bed temperature.

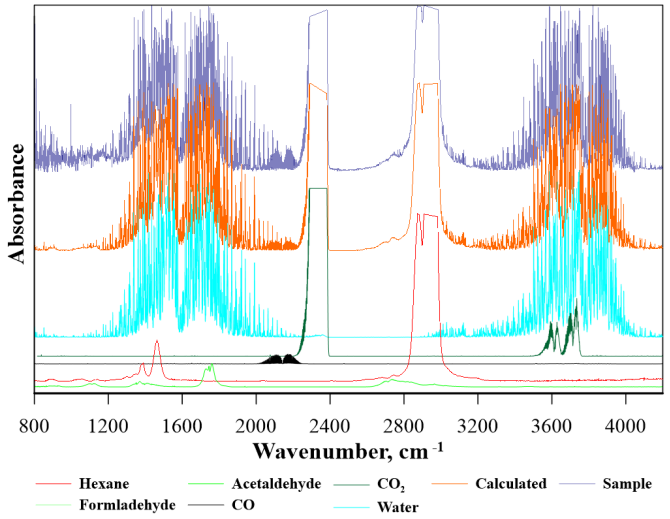

Figure 6. FTIR spectra during catalytic conversion of hexane on Ag/Fe_2O_3/C catalyst at 350 °C.

The decomposition of isopropanol on the Fe_2O_3/C catalyst (Fig. 7A) begins below 200 °C. This is evidenced by the presence of acetone in the exhaust gases. The concentration of this product reaches a maximum at approximately

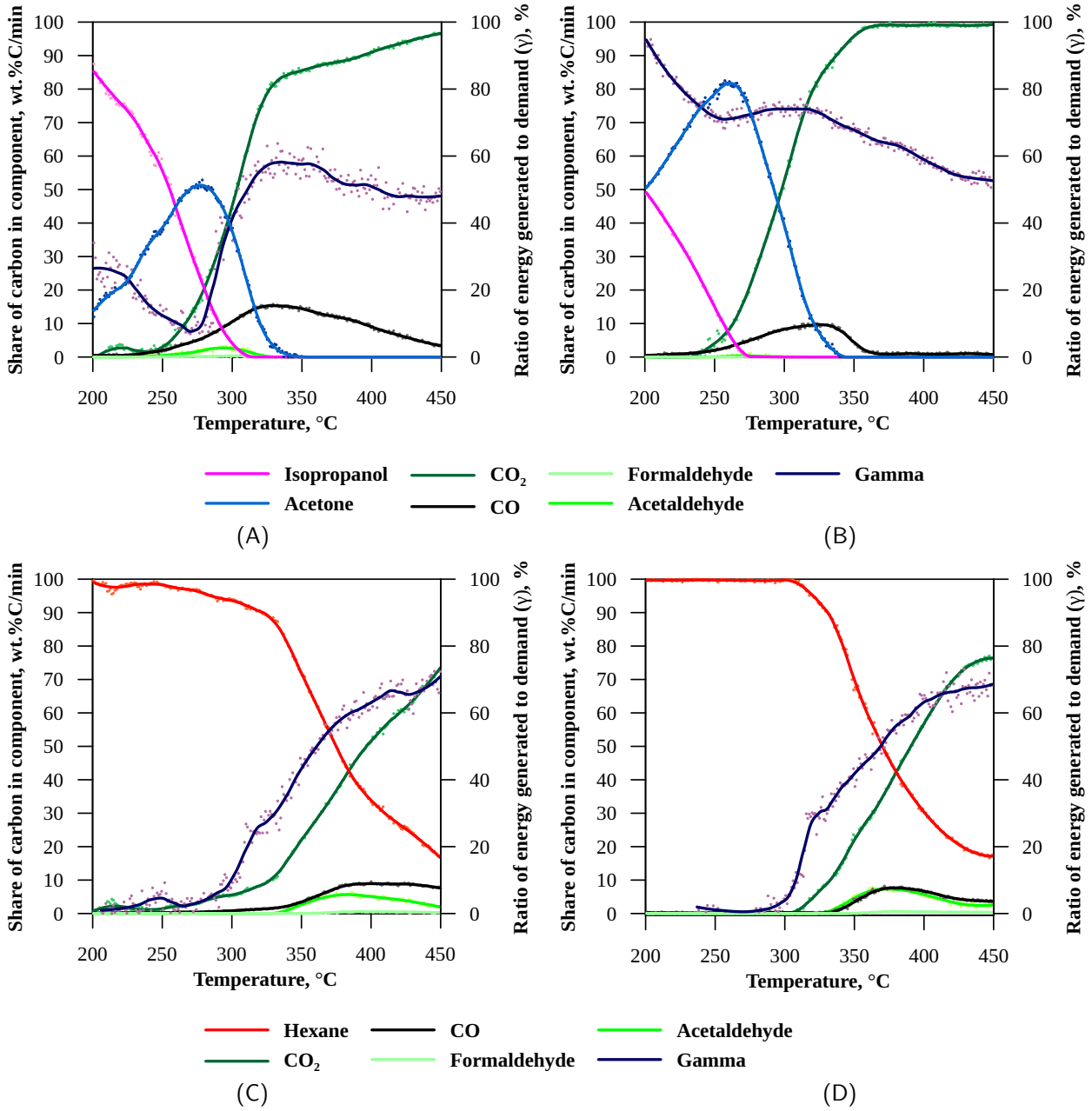

Figure 7. Results of the catalytic oxidation experiments: A) IPA-Fe_2O_3/C B) IPA-Ag/Fe_2O_3/C, C) HEX-Fe_2O_3/C D) HEX-Ag/Fe_2O_3/C.

275 °C. From a temperature of ∼ 315 °C, isopropanol is not present in the exhaust gases, but the process of complete oxidation of CO to carbon dioxide takes place at temperatures above 450 °C. Other components of incomplete decomposition of isopropanol (formaldehyde and acetaldehyde) are present especially in the temperature range of 250–320 °C, while above 350 °C the only product of incomplete combustion is CO. The ratio of heat generated during the reaction to the energy demand (γ) does not exceed 60%. In the range of 200–230 °C γ reduction is observed, which is caused by the endothermic reaction of acetone formation, whereas the rise of γ coefficient above 230 °C results from an increase in the reaction rate of acetone oxidation.

The process carried out on the Ag/Fe_2O_3/C catalyst has a similar nature (Fig. 7B). However, there is a noticeable increase in the rate of reactions taking place in the fluidized bed reactor. The maximum acetone concentration is at approximately 260 °C, isopropanol is not present in the gases above 275 °C, and the CO combustion process is almost completed at ∼ 375 °C. The Ag implementation also led to a significant reduction in the concentration of aldehydes in the process gases. The process of catalytic oxidation of isopropyl alcohol during tests with Ag/Fe_2O_3/C catalyst, is characterised by improved energy ballance in comparision to the process with Fe_2O_3/C. The value of γ exceeds 90% at 200 °C, when isopropyl alcohol conversion is ∼ 50%, whereas at complete isopropanol conversion to CO_2 (375 °C) this coefficient value is ∼ 60%.

The decomposition of hexane on the Fe_2O_3/C catalyst (Fig. 7C) starts at a temperature of approximately 250 °C and initially the main decomposition product is carbon dioxide. Starting from a temperature of ∼ 320 °C, higher concentrations of CO appear, along with formaldehyde and acetaldehyde, which, similarly to hexane, are not completely converted even at 450 °C. The introduction of silver to the catalyst (Fig. 7D) did not significantly affect the catalytic oxidation of hexane, which may indicate that silver is not catalytically active in this process.

This observation is confirmed by quantitative data of the degree of hexane decomposition (Table 1). According to these data, for the Fe_2O_3/C catalyst, the hexane concentration is equal to 75% of the initial value at 346.5 °C and 25% at 427.5 °C. The introduction of silver lowered these temperatures, but only to a small extent. However, the decomposition of isopropanol requires much lower conversion temperatures than hexane, because in the case of the Fe_2O_3/C catalyst only 25% of isopropanol remains at 276.3 °C. Carrying out the process over the Ag/Fe_2O_3/C catalyst led to a significant reduction in the isopropanol decomposition temperature ($T25\% = 238$ °C), confirming the catalytic effect of silver. There were no singnificant differences observed between γ values during catalytic conversion of hexane depending on the catalyst used. In both cases γ started to rise above certain temperature when hexane conversion began and reached the maximum value of ∼ 70% at 450 °C.

Table 1. Comparison of the degree of pollutant decomposition depending on process temperatures and the catalyst used.

Sample	Type of VOCs	Temperature of residual VOC mass content		
		T 75% [°C]	T 50% [°C]	T 25% [°C]
Fe_2O_3/C	Hexane	346.5	375.0	427.5
Ag/Fe_2O_3/C	Hexane	346.0	370.1	411.5
Fe_2O_3/C	Isopropanol	220.8	256.4	276.3
Ag/Fe_2O_3/C	Isopropanol	<200	<200	238.0

3.5. Results of toxicity evaluation

Toxicity analysis of the reactor exhaust gases generated during the catalytic combustion of isopropanol (Figs. 8–10) revealed differences between the catalysts used. The calculated gas toxicity at 200 °C was approximately 2 m^3/g of gas and was related to the presence of isopropanol, but also acetone, carbon monoxide, and carbon dioxide. At this temperature, the contribution of isopropanol to the total toxicity of the gases was 85% and 52% for the Fe_2O_3/C and Ag/Fe_2O_3/C catalysts, respectively. This indicates that the catalytic effect of silver was observed starting from the low temperatures of the process. At higher temperatures, the toxicity of gases for the Fe_2O_3/C catalyst was mainly caused by the presence of formaldehyde, which has the lowest TLV-TWA index among the tested substances (0.1 ppm). On the other hand, the use of the Ag/Fe_2O_3/C bed contributed to reduced formaldehyde emissions. For both catalysts, the maximum emission of this component occurred at approx. 300 °C. Hence, the maximum toxicity values were 17.5 m^3/g of gases (∼ 305 °C) for the Fe_2O_3/C catalyst and 4.2 m^3/g of gases (∼ 295 °C) for the Ag/Fe_2O_3/C catalyst. The analysis of the toxicity of the gaseous products shows that in the initial stage of the process its value increases with increasing temperature up to approx. 300 °C and then decreases. In the case of the Fe_2O_3/C bed, the toxicity decreases (to a level lower than at the beginning of

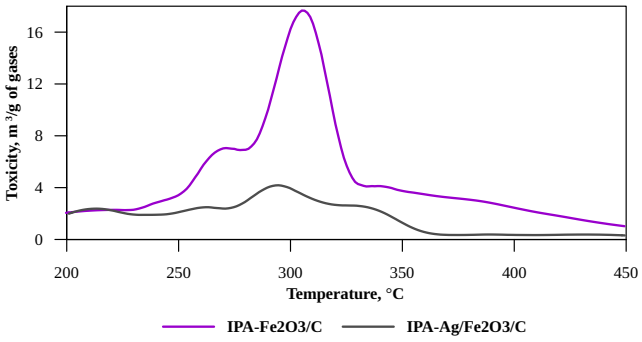

Figure 8. Comparison of the toxicity of gases produced in the process of catalytic oxidation of isopropanol.

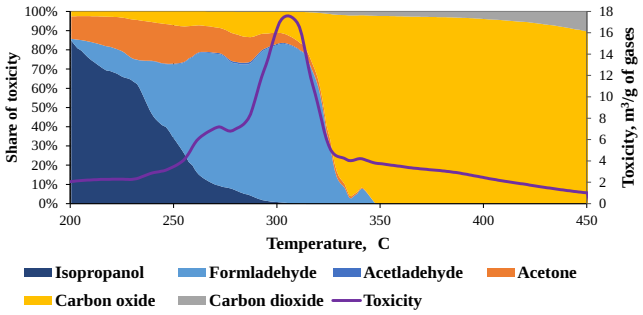

Figure 9. The influence of individual components on the toxicity of gases in the process of catalytic oxidation of isopropanol on a Fe_2O_3/C catalyst.

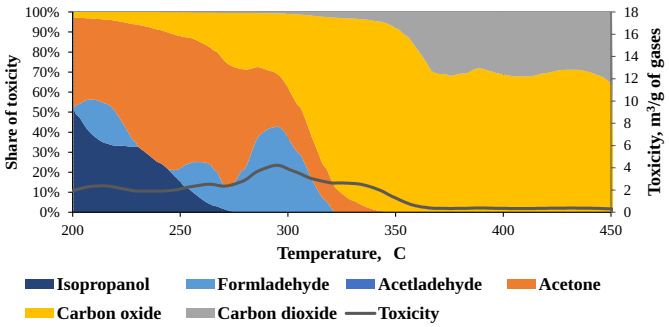

Figure 10. The influence of individual components on the toxicity of gases in the process of catalytic oxidation of isopropanol on a Ag/Fe_2O_3/C catalyst.

the process) only at temperatures above 400 °C. However, the $Ag/Fe_2O_3/C$ catalyst requires a temperature of about 370 °C to almost completely reduce the toxicity of the gases produced; notably, above this temperature the toxicity is caused by residual CO. Therefore, it can be concluded that the addition of silver caused both an acceleration of the reaction (lower share of isopropanol at 200 °C) and a change in the mechanism of the process (lower share of formaldehyde). It is also worth noting that in the case of the $Ag/Fe_2O_3/C$ bed, there is a sharp decrease in CO concentration in the temperature range of 340–365 °C (Fig. 10). This may indicate that the used catalyst also has a beneficial effect on the oxidation of CO to CO_2. It is certainly not the optimal catalyst for this process, as the CO concentration remains constant at higher temperatures.

A similar analysis of the toxicity of the hexane oxidation process showed that there are no significant differences between the catalytic beds used (Figs. 11–13). Both the total toxicity of gases and the contribution of individual components over the entire range of tested temperatures are similar in both cases. Hexane decomposition at temperatures above 350 °C produces a gas mixture with a toxicity higher than the initial value. The gas toxicity at the beginning of the experiment (200 °C) was approximately 6 m^3/g of gas and was primarily due to the presence of hexane itself. Up to a temperature of approximately 340 °C, hexane contributed approximately 90% to the total toxicity. At higher temperatures, when the significant decomposition of hexane began, the toxicity of the decomposition products was higher than the initial value, reaching a maximum value of approximately 24 m^3/g of gas. Detailed data indicate that formaldehyde is primarily responsible for the toxicity, accounting for 80% of the total toxicity at 450 °C. This analysis clearly indicates that the catalysts used, both Fe_2O_3/C and $Ag/Fe_2O_3/C$, are not suitable for the hexane oxidation process at the tested temperatures and the residence time applied in the fluidized bed. Despite the activity of the catalysts and the significant reduction in the hexane concentration in the gases, the resulting gases containing CO, CO_2 and aldehydes were more toxic than hexane.

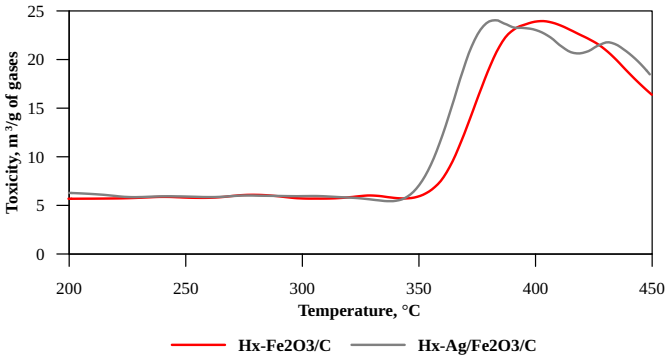

Figure 11. Comparison of the toxicity of gases produced in the process of catalytic combustion of hexane.

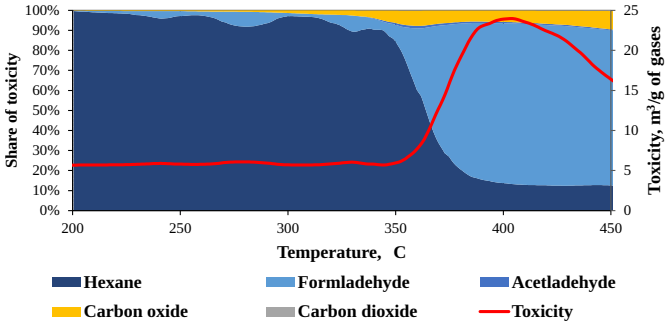

Figure 12. The influence of individual components on the toxicity of gases in the process of catalytic oxidation of hexane on a Fe_2O_3/C catalyst.

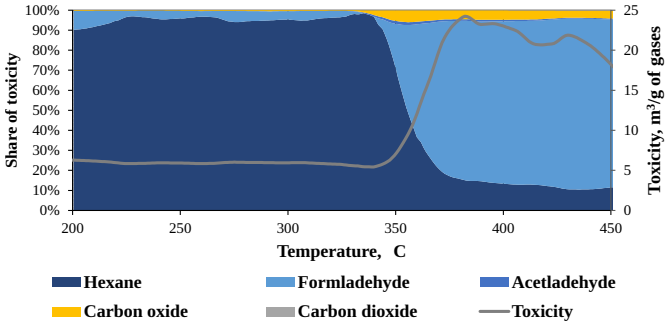

Figure 13. The influence of individual components on the toxicity of gases in the process of catalytic oxidation of hexane on a $Ag/Fe_2O_3/C$ catalyst.

4. CONCLUSIONS

- Spherical, mechanically and thermally durable cenospheres with low density allow for operation in a fluidized state at elevated temperatures and at linear gas velocity lower than those for conventional quartz sand beds. The cenosphere support also enables the creation of a core-shell catalyst in which the catalyst layer is covered only on the outer surface of the cenosphere, resulting in reduced use of the active ingredient.
- In this study two core-shell catalysts were obtained in which hematite (Fe_2O_3/C) and hematite with metallic silver ($Ag/Fe_2O_3/C$) were deposited on the outer surface of the cenospheres. SEM/EDS analysis showed a uniform distribution of the Fe_2O_3 phase on the cenosphere surface, indicating that the MO-CVD method was suitable for applying the iron coating. In turn, Ag particles formed larger agglomerates, up to several micrometers in size, which still covered almost the entire cenosphere surface. Therefore, the use of ion exchange proved to be less advantageous than the gas deposition process. On the other hand, the coating obtained was mechanically durable and exhibited catalytic properties.
- The toxicity of exhaust gases during the initial stage of pollutant decomposition increased with increasing process temperature, after which it gradually decreased. However, the use of an $Ag/Fe_2O_3/C$ catalyst in the isopropanol

combustion process enables the reduction of toxicity to negligible values at 370 °C, which indicates the favorable effect of silver in eliminating this pollutant. However, the research did not confirm the benefits of using silver during hexane combustion. Although > 80% decomposition of pollutant occurs at 450 °C for both the Fe_2O_3/C and Ag/Fe_2O_3/C catalysts, the resulting gaseous components are more toxic than hexane itself.

ACKNOWLEDGMENTS

This research was funded by National Science Center – Poland, grant number 2022/06/X/ST8/00628.

SYMBOLS

W	Toxicometric index, the standardized volume of toxic gases (m^3) emitted from the thermal decomposition or combustion of 1 mg of sample, m^3/mg of sample
E	Specific emission of selected gaseous component, g/g of sample
E_T	Toxicity, sum of toxicometric indices for a continuous process, m^3/g of gases
TLV–TWA	Threshold Limit Values in order of 8-hour time weighted averages, maximum permissible concentration that does not cause adverse health effects during 8 hours of exposure in the workplace, mg/m^3
u_{mf}	Minimum fluidization velocity, cm/s
u	Superficial velocity, cm/s
$\Delta_f H^0_{\text{gas}\,i}$	Enthalpy of selected compound formation in the gaseous state, J/kg
$\dot{m}_i(t)$	Mass flow rate (as function of time) of selected compound, kg/s
$\dot{m}_{\text{Air}}$	Mass flow rate of air, kg/s
$Q_{\text{react.}}(t)$	Heat generated at time t during catalytic oxidation of selected compound, W
$C_{p\,\text{Air}}(T)$	Heat capacity of air at constant pressure as temperature function, J/(kg·K)
$T(t)_{\text{Bed}}$	Temperature of the fluidized bed at time t, °C
γ	Ratio between heat generated during reaction and heat demand for heating, %

REFERENCES

ACGIH, American Conference of Governmental Industrial Hygienists. *TLVs and BEIs: Threshold limit values for chemical substances and physical agents and biological exposure indices*. Available at: https://www.acgih.org/science/tlv-bei-guidelines/documentation-publications-and-data.

Berkowicz-Płatek G., Żukowski W., Leski K., 2024. Production of hydrogen from polyoxymethylene in a binary fluidized bed. *Appl. Energy*, 360, 122833. DOI: 10.1016/j.apenergy.2024.122833.

Chauveau R., Grévillot G., Marsteau S., Vallières C., 2013. Values of the mass transfer coefficient of the linear driving force model for VOC adsorption on activated carbons. *Chem. Eng. Res. Des.*, 91, 955–962. DOI: 10.1016/j.cherd.2012.09.019.

Engineering ToolBox. Available at: https://www.engineering toolbox.com/.

Guo Y., Yang D.-P., Liu M., Zhang X., Chen Y., Huang J., Li Q., Luque R., 2019. Enhanced catalytic benzene oxidation over a novel waste-derived Ag/eggshell catalyst. *J. Mater. Chem. A*, 7, 8832–8844. DOI: 10.1039/C8TA10822F.

He C., Cheng J., Zhang X., Douthwaite M., Pattisson S., Hao Z., 2019. Recent advances in the catalytic oxidation of volatile organic compounds: a review based on pollutant sorts and sources. *Chem. Rev.*, 119, 4471–4568. DOI: 10.1021/acs.chemrev.8b00408.

He C., Yue L., Zhang X., Li P., Dou B., Ma C., Hao Z., 2012. Deep catalytic oxidation of benzene, toluene, ethyl acetate over Pd/SBA-15 catalyst: reaction behaviors and kinetics. *Asia-Pac. J. Chem. Eng.*,7, 705–715. DOI: 10.1002/apj.621.

Jurkiewicz M., Musik M., Pełech R., 2023. The effect of fixed adsorption bed height on adsorption of gaseous mixture of volatile organic compounds. *Chem. Process Eng.*: *New Frontiers*, 44, e47. DOI: 10.24425/cpe.2023.147406.

Kang J., Wang Z., Yang Z., Yan Y., Ran J., Guo M., 2020. Catalytic combustion of low concentration Methane over Mx-Cu/γ-Al_2O_3 (M = Mn/Ce) catalysts. *Ind. Eng. Chem. Res.*, 59, 4291–4301. DOI: 10.1021/acs.iecr.9b06203.

Kim H.-S., Kim H.-J., Kim J.-H., Kim J.-H., Kang S.-H., Ryu J.-H., Park N.-K., Yun D.-S., Bae J.-W., 2022. Noble-metal-based catalytic oxidation technology trends for volatile organic compound (VOC) removal. *Catalysts*, 12, 63. DOI: 10.3390/catal12010063.

Miao L., Wang J., Zhang P., 2019. Review on manganese dioxide for catalytic oxidation of airborne formaldehyde. *Appl. Surf. Sci.*, 466, 441–453. DOI: 10.1016/j.apsusc.2018.10.031.

Migas P., Żukowski W., Bradło D., 2023. Catalytic oxidation of volatile organic compounds using the core–shell Fe_2O_3-cenospheric catalyst in a fluidised bed reactor. *Energies*, 16, 2801. DOI: 10.3390/en16062801.

NIOSH, National Institute for Occupational Safety and Health. *NIOSH Pocket Guide to Chemical Hazards*. Available at: https://www.cdc.gov/niosh/npg/.

NIST Chemistry WebBook. Available at: https://webbook.nist.gov/chemistry/name-ser/.

OSHA, Occupational Safety and Health Administration. *Occupational Chemical Database*. Available at: https://www.osha.gov/chemicaldata.

Ranjbar N., Kuenzel C., 2017. Cenospheres: a review. *Fuel*, 207, 1–12. DOI: 10.1016/j.fuel.2017.06.059.

Rybarczyk P., 2022. Removal of volatile organic compounds (VOCs) from air: focus on biotrickling filtration and process modeling. *Processes*, 10, 2531. DOI: 10.3390/pr10122531.

Rybarczyk P., Szulczyński B., Dobrzyniewski D., Kucharska K., Gębicki J., 2023. Removal of cyclohexane vapors from air in biotrickling filters: Effects of gas mixture composition and circular economy approach. *Chem. Process Eng.*: *New Frontiers*, 44, e40. DOI: 10.24425/cpe.2023.147399.

Rybiński P., Syrek B., Szwed M., Bradło D., Żukowski W., Marzec A., Śliwka-Kaszyńska M., 2021. Influence of thermal decomposition of wood and wood-based materials on the state of the atmospheric air. Emissions of toxic compounds and greenhouse gases. *Energies*, 14, 3247. DOI: 10.3390/en14113247.

Scirè S., Minicò S., Crisafulli C., Galvagno S., 2001. Catalytic combustion of volatile organic compounds over group IB metal catalysts on Fe_2O_3. *Catal. Commun.*, 2, 229–232. DOI: 10.1016/S1566-7367(01)00035-8.

Tabakova T., Grahovski B., Karakirova Y., Petrova P., Venezia A.M., Liotta L.F., Todorova S., 2025. Effect of support on complete hydrocarbon oxidation over Pd-based catalysts. *Catalysts*, 15, 110. DOI: 10.3390/catal15020110.

Todorova S., Naydenov A., Kolev H., Holgado J.P., Ivanov G., Kadinov G., Caballero A., 2012. Mechanism of complete n-hexane oxidation on silica supported cobalt and manganese catalysts. *Appl. Catal., A: Gen.*, 413–414, 43–51. DOI: 10.1016/j.apcata.2011.10.041.

Wen C.Y., Yu Y.H., 1966. Mechanics of fluidization. *Chem. Eng. Prog. Symp. Ser.* 162, 100–111.

Zhang X., Song L., Bi F., Zhang D., Wang Y., Cui L., 2020. Catalytic oxidation of toluene using a facile synthesized Ag nanoparticle supported on UiO-66 derivative. *J. Colloid Interface Sci.*, 571, 38–47. DOI: 10.1016/j.jcis.2020.03.031.

Żukowski W., Berkowicz G., 2019a. The combustion of polyolefins in inert and catalytic fluidised beds. *J. Cleaner Prod.*, 236, 117663. DOI: 10.1016/j.jclepro.2019.117663.

Żukowski W., Berkowicz G., 2019b. The combustion of liquids and low-density solids in a cenospheric fluidised bed. emph-Combust. Flame, 206, 476–489. DOI: 10.1016/j.combustflame.2019.05.024.

Żukowski W., Migas P., Żurek M., Wrona J., 2023. Catalytic oxidation of n-hexane in a fluidized bed with modified flow. *J. Cleaner Prod.*, 402, 136848. DOI: 10.1016/j.jclepro.2023.136848.